Paper 29

A Finite Element Study of the Severe Temperature Effect on the Behaviour of Elliptical Hollow Section Columns

N. Goodfellow[1], F. Ali[1], T. Scullion[1], A. Nadjai[1] and J. Gardner[2]
[1] FireSERT, School of the Built Environment
  University of Ulster, Newtownabbey, United Kingdom
[2] Jeremy Gardner Associates
  London, United Kingdom

Abstract

This paper presents the first ever validated finite element study on steel columns with elliptical hollow sections (EHS) subjected to severe hydrocarbon fire temperatures reaching 900°C in the first 4 minutes of heating. A three-dimensional model was built using the finite element method (FEM) and the results were validated using specially conducted experiments on axially restrained elliptical columns. By using variable with temperature thermal expansion coefficient and the EC3 thermal parameters, the finite element model demonstrated an excellent agreement with experimental results including failure temperatures, failure modes, axial displacements and the generated axial forces. The experimental data was obtained from fire tests performed on 12 steel columns with elliptical sections investigating structural parameters including loading level and axial restraint. The verified finite element model was used to conduct a parametric analysis involving a range of parameters of loading level and slenderness. The study has shown a non-linear relationship between the loading ratio and slenderness of elliptical columns and that the load ratio has more effect on failure time on columns with high slenderness.

Keywords: finite element, fire, elliptical, hydrocarbon, steel, restraint.

1   Introduction

Elliptical steel hollow sections present a recent addition to the range of steel sections available to structural engineers. However, despite the extensive interest in their use due to their aesthetically pleasing shape, particularly by architects, there is currently a lack of dedicated studies on their structural performance under high temperatures inhibiting more widespread use in construction particularly in fire situations. Previous studies carried out to date have concerned the testing and analysis of steel columns with elliptical hollow sections under normal temperatures. The initial

research programme was carried out by Imperial College which involved experimental testing, involving stub columns and a finite element study. The paper by Chan and Gardner [1] used the finite model software ABAQUS which was able to produce good agreement with the test data and failure modes for the stub columns under ambient conditions. The validated model was used to conduct parametric analyses which give rise to the guidance on the classification of EHS. Zhu and Wilkinson [2] also used ABAQUS to model elliptical hollow sections for stub columns in order to predict an equivalent Circular Hollow Sections (CHS) which provided an overall understanding of local buckling behaviour of EHS and CHS. Following on from this a paper by Jamaluddin et al [3] investigated the performance of elliptical sections filled with concrete also using ABAQUS and was validated using some of the test data from Imperial College to validate the models use in composite form. The results from the modelling showed some agreement with the tests but further work was needed to refine the model further under loading conditions. It is obvious from the available literature that a limited amount of research has involved the modelling of elliptical sections under fire conditions especially under the hydrocarbon fire curve and none of the previous studies was validated with experimental data obtained from fire tests. This paper presents a finite element study on the performance of EHS under hydrocarbon fire temperatures with validation provided by comparing the results with tests carried out at FireSERT at the University of Ulster. The paper also presents the experimental data (including measured temperatures, displacements and failure time) obtained from the fire tests which involved 12 steel columns with elliptical sections. The paper is therefore leading the way into such areas in order to highlight the issues that may arise in the performance of EHS under fire situations and address the issues when using Finite Element Modelling to analyse and predict the structural behaviour of oval sections. The hydrocarbon fire curve with upper and lower limits which was used in the finite element study is shown in Figure 1 and taken from EC1 [4].
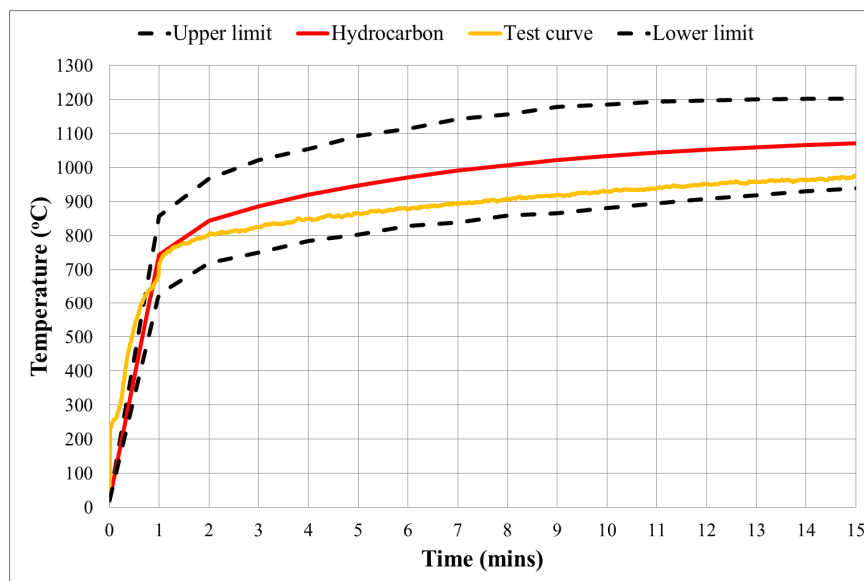

Figure 1: Hydrocarbon fire curve with upper and lower limits

2

2   The Finite Element Model

2.1   Temperature Analysis

The elliptical columns were modelled using the finite element method and the software Diana TNO [5]. The program is capable of a wide range of calculation aspects which includes temperature and structural analysis. In analysing the thermal response of the columns, a transient heat transfer analysis was performed using a three-dimensional steady-state heat flow derived for the Law of Conservation of Energy:

$$\frac{\delta}{\delta x}\left(k\frac{\delta T}{\delta x}\right)+\frac{\delta}{\delta y}\left(k\frac{\delta T}{\delta y}\right)+\frac{\delta}{\delta z}\left(k\frac{\delta T}{\delta z}\right)+Q-\rho c\frac{\delta T}{\delta t}=0 \tag{1}$$

where: k is the thermal conductivity; T is the temperature gradient; Q is the internally generated heart per unit volume per unit time, ρ is the density of the material; c is the specific heat of the material and t is time. Solution of equation (1) is governed by the boundary condition:

$$-k\frac{\delta T}{\delta n}=h_{c}\left(T_{s}-T_{f}\right)+h_{r}\left(T_{s}-T_{f}\right) \tag{2}$$

where: n is the direction of heat flux; h_c is the heat transfer coefficient; T_s is the temperatures of the solid surface, T_f is the temperatures of the fluid and h_r is the radiation heat transfer coefficient calculated using Stefan-Boltzmann equation.

The Galerkin method was used by determining {T} as a function of time and expressed as the first order differential equation:

$$[k]\{T_{n}\}+[c]\{T_{n}\}=\{F_{n}\} \tag{3}$$

where: [k] is element heat conduction/convection matrix; [c] is element heat capacity matrix; $\{T_n\}$ is element nodal temperature vector; $\{F_n\}$ is element nodal heat input vector and defined at boundary nodes using equation (4):

$$-k\left[\frac{\delta T}{\delta x}l_{1}+\frac{\delta T}{\delta x}m_{1}\right]=h_{c}\left[T_{e}-T_{r}\right]+\varepsilon_{e}\sigma\left[T_{e}^{4}+T_{r}^{4}\right] \tag{4}$$

where: T_e = temperature of emitting surface; T_r = temperature of surface; s = Stefan-Boltzmann coefficient; l_1 -direction cosine of n relative to x = cos θ; m_1 = direction cosine of n relative to y = sin θ; ε_e = emissivity of the surface.

2.2 Structural Analysis

After completing the thermal analysis, the model undergoes structural analysis to evaluate the effect of temperatures on the column behaviour. The stresses that occur under temperature are governed by the following equation:

$$\{\sigma\} = [K]\{\varepsilon - \varepsilon_T\} \qquad (5)$$

where: $\{\sigma\}$ = stress vector; [K] = stiffness matrix; ε_T = thermal strain vector

2.3 Model Material

In order to calculate the stiffness matrix [K] in equation (5) a material model was assigned to the structural element. In the case of the elliptical section it is taken as steel material with a yield stress value of $355N/mm^2$, a standard stress/strain curve is adapted with the Von-mises failure criteria used. The non-linear properties of the steel are taken from EC3 [7] for the change due to high temperatures.

2.4 The Created Model

A 3-D model was built for 2 elliptical sections, 200x100x8mm and 250x125x8mm, providing slenderness ratios, λ = 51 and 40 respectively. The column structural model consists of a 20 node iso-parametric brick element, CHX60, [5] which allows for three degrees of freedom and estimates the stress and strain of the material through the volume of the element using a 3x3x3 integration system based on Gauss integration. The boundary heated element, BQ4HT, (which is a four-node iso-parametric quadrilateral element) was used to describe boundaries in three-dimensional general potential flow analysis [5]. It is based on linear interpolation and Gauss integration. During the analysis stage the twenty-node iso-parametric brick element is merged with the 4 nodes of the three-dimensional (3D) linear boundary flow element. A sensitivity analysis was carried out in order to determine the optimum size of meshing to be used to achieve fast computational time without compromising on the performance of the model. The final model created consisted of 38845 nodes and 10445 elements that represent the structural and temperature elements as shown in Figure 2. The room temperature compressive capacity of the model was first validated using the EC3 [6], before a structural thermal analysis was commenced. The numerical analysis was performed using a staggered transient heat-flow stress path. The built model considered thermal conduction and radiation heat transfer. The heat transfer analysis produces nodal temperature readings which are used in the structural analysis to determine the reduction in the yield strength and stiffness of the steel material properties according to EC3 along the length of the column.
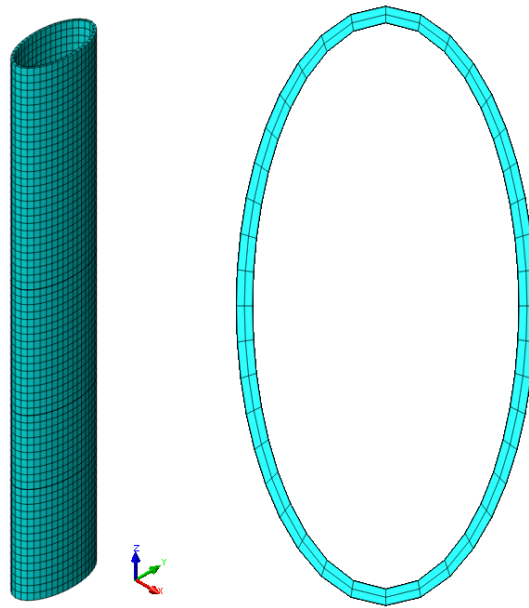
4

Figure 2: FEM created for the elliptical sections

Before the structural nonlinear analysis was carried out the model underwent a structural stability check that involves an Eigenvalue analysis taking into account any imperfections and loading eccentricities. This produces predicted buckling failure modes that will occur either by local, overall or a combination of both. The temperature values resulting from the heat flow analysis were then tabulated into a time-temperature form, and used for the structural analysis. During the structural analysis the boundary element was deactivated, and the potential flow element was converted to the three-dimensional twenty node iso-parametric solid brick structural element. The nonlinear structural analysis is run with Newton Modified method with line search algorithm used to solve the system of equations.

2.5 Axial Restraint

In the case of considering axial restraint being applied to the columns, the restraint was modelled using a one way spring with constant stiffness to simulate the effect of surrounding structural elements in practice. The restraint is formed by using a 0D, one node element in the form of a discrete spring/dashpot element, SP1TR, whereby the total restraint applied is the total number of nodes times the individual spring stiffness of each node. The model allows for the loading and unloading of the spring to occur (Figure 3) so as to accommodate the mechanical loading on the column. This was specified in the analysis by in putting two spring diagrams one of which is where there is no spring present and the other representing the stiffness of the surrounding structure.
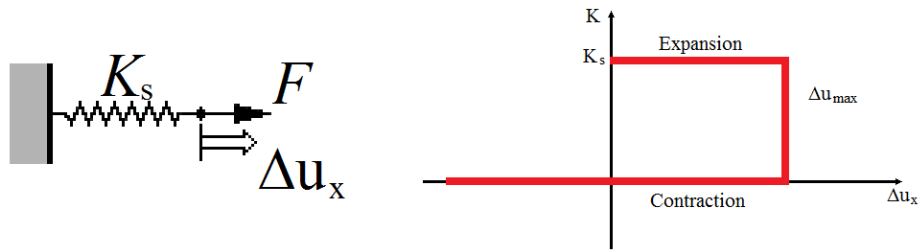
Figure 3: Spring unloading and reloading used in modelling

3   Validation of the Model - Test Programme

In order to validate the model output an innovative testing program was carried out at the University of Ulster FireSERT to investigate the performance of elliptical hollow steel (EHS) columns under the extreme hydrocarbon fire curve. The test program included testing 12 columns of various section sizes and slenderness values under different loading levels and different degrees of axial restraint. The tests were carried out on 2 EHS sections 200x100x8mm (EHS-A) and 250x125x8mm (EHS-B) yielding 2 slenderness ratios of λ = 51 and 40. All columns were 1800mm in length and were pinned at both ends. All the columns were subjected to a hydrocarbon fire curve under different loading levels ranging from 0.2 to 0.6 of the EC3 ultimate strength and were subjected to axial restraint degrees ranging from 0 (unrestrained) to 0.12 (degree of axial restraint = applied stiffness/column's axial stiffness). The results from the tests are summarised in Table 1 for unrestrained tests and Table 2 for the restrained tests.

Section	λ	Load Ratio	Load (kN)	Maximum Displacement (mm)	Time of Failure (mins)
EHS-A.0.2		0.2	208	10.52	14
EHS-A.0.4	50.85	0.4	417	7.30	10
EHS-A.0.6		0.6	625	5.50	8
EHS-B.0.3		0.3	400	8.52	14
EHS-B.0.45	40.09	0.45	600	6.75	12
EHS-B.0.6		0.6	800	5.12	10

EHS-A	EHS-B

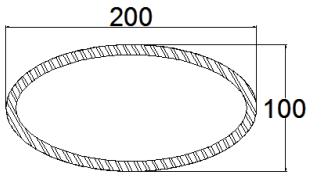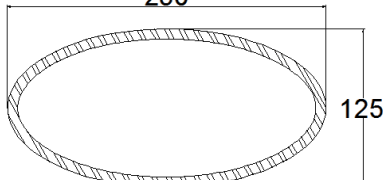Table 1: Summary of test results for unrestrained columns

Section	λ	Load Ratio	Load (kN)	Degree of Axial Restraint	Restraint Force (kN)	Maximum Displacement (mm)	Time of Failure (mins)
EHS-AR.0.2		0.20	208		257	5.02	10
EHS-AR.0.4	50.85	0.40	417	0.120	186	4.00	8
EHS-AR.0.6		0.60	625		101	2.46	5
EHS-BR.0.3		0.30	400		349	5.51	12
EHS-BR.0.45	40.09	0.45	600	0.116	291	4.35	11
EHS-BR.0.6		0.60	800		208	3.31	10

EHS-A	EHS-B

Table 2: Summary of test results for restrained columns

4   Validation of the Finite element model

4.1 Unrestrained Columns

The output from the modelling provides detailed predictions on the temperature and deformation of the sections over the period that is exposed to the fire. Figure 4 shows that for the EHS-A the FEM is in good agreement with the tests with regards to the failure time and the max displacement. A slight divergence is noticeable under low loading on the displacement domain; however agreement was obtainable in the failure time domain. With regards to the larger EHS-B results in Figure 5 there is good agreement with respect to the failure times with slight divergence noticed in the axial deformation. This slight divergence is more evident in the high loading scenario.

The failure mechanism that was observed in the testing was generally overall buckling of the elliptical columns. However there is evidence of local buckling occurring also at the failure point along with the overall buckling. The developed model has also shown excellent agreement with the test results in relation with the local and overall buckling failure modes as shown in Figures 6 and 7.
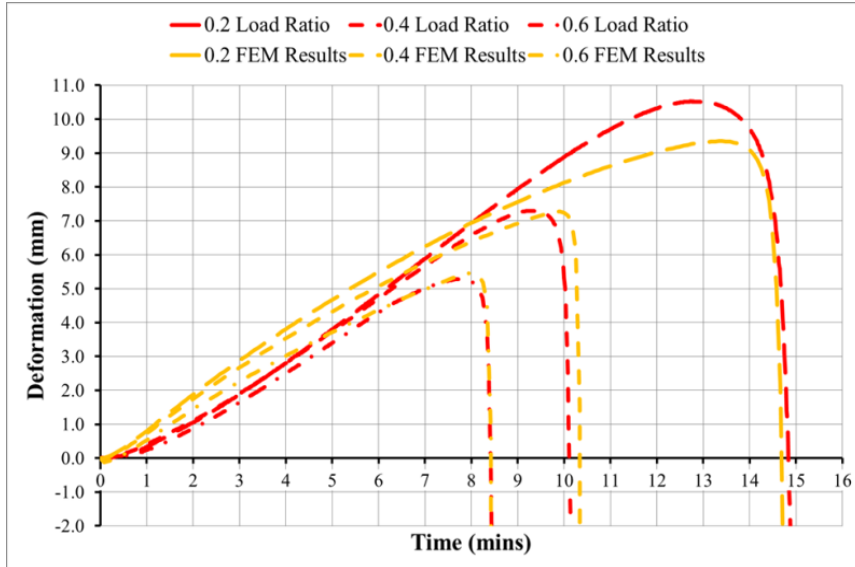
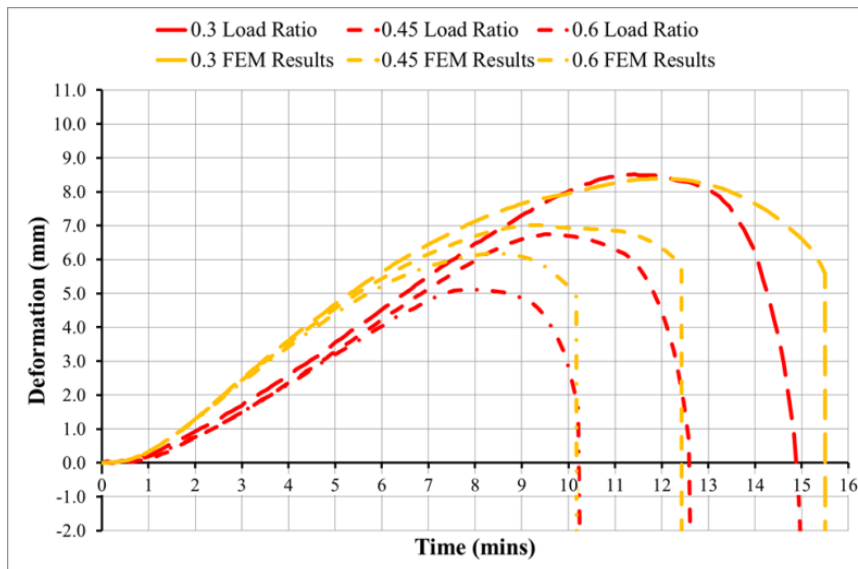Figure 4: Time v Deflection for test results and FEM for EHS-A

Figure 5: Time v Deflection for test results and FEM for EHS-B
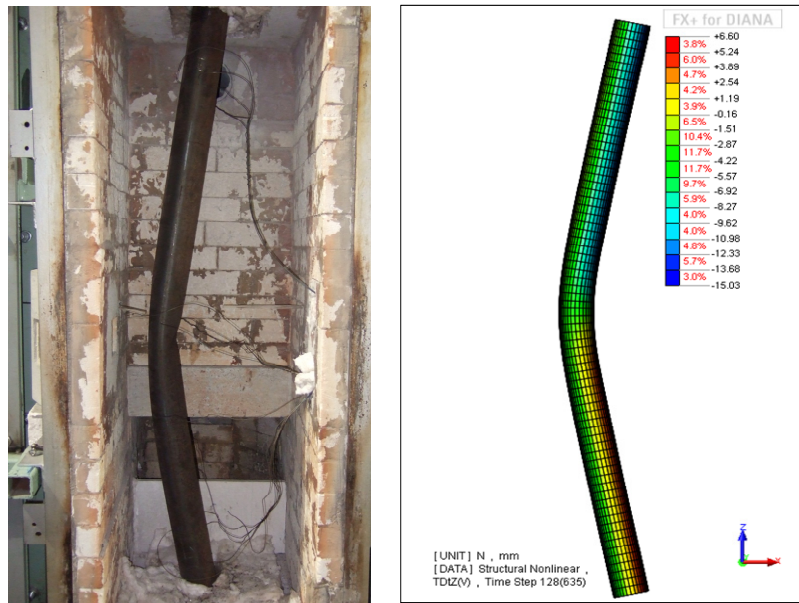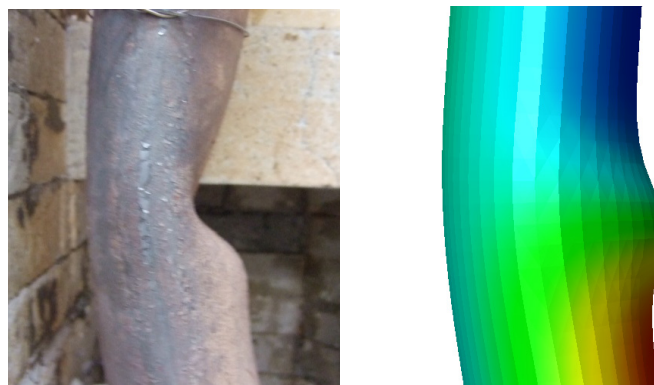
8

Figure 6: Test and FEM failure mechanism

Figure 7: Test and FEM local buckling failure mechanism

4.2 Restrained Columns

The models used for the unrestrained columns were then subjected to a restraining force that would represent any surrounding structure which in this case is the testing rig. The summary of the results are shown in Table 3 for the restraint scenario. It can be seen that there is excellent agreement between the tests and FEM in regards to the failure time and maximum displacements with some small divergence seen when the

9

load increases to 0.6 of the ultimate load. It was noted that the model failure occurs rather rapidly once the maximum displacement was reached in comparison to the tested columns where failure was gradual especially in the case for the higher loads. The results from the FEM and the tests for the restraint case showed excellent correlation to the failure time and maximum axial displacement as well as excellent agreement into the failure mechanism which was similar to that of the unrestrained results.

Section	Load Ratio	Degree of Axial Restraint	Maximum Displacement (mm)		Time of Failure (mins)	
			FEM	Exp	FEM	Exp
EHS-AR.0.2	0.20		5.62	5.02	9	10
EHS-AR.0.4	0.40	0.120	4.67	4.00	7	8
EHS-AR.0.6	0.60		2.99	2.46	6	5
EHS-BR.0.3	0.30		5.42	5.51	12	12
EHS-BR.0.45	0.45	0.116	4.90	4.35	10	11
EHS-BR.0.6	0.60		4.44	3.31	9	10

Table 3: Summary of results for FEM and Experiment restraint tests.

5   Parametric Analysis

With the model verified by the test results a parametric analysis has been carried out on one of the models for the unrestrained EHS-B column. The analysis studied the effect of different load levels, of the varying slenderness values 60, 90 and 120 on uniformly heated sections. The maximum load for each of the columns was calculated using EC3 method and an initial imperfection of L/360 was applied to each of the columns. The result from the analysis for λ=90 is shown in Figure 8 with the summary shown in Figure 9; which shows that the more slender the column is the lower the failure temperature is for the section. Figure 8 shows also that increasing the loading level form 0.2 to 0.8 has reduced the maximum displacement by 47 % and decreased the failure temperature by 28%. Figure 9 clearly shows a non-linear relationship between the loading ratio and the slenderness of the elliptical columns. In slenderness range of 90 to 120 the effect of loading on failure temperature is less than that in the range of 60 to 90. However in loading levels higher than 70% the reduction in failure temperatures is more significant in columns with slenderness around 120.
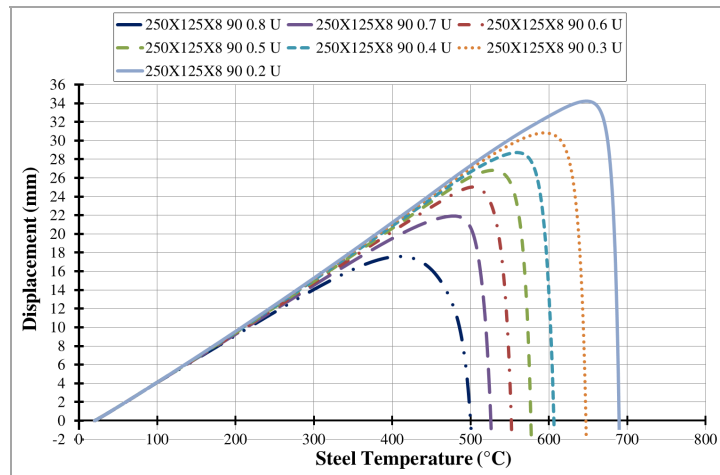
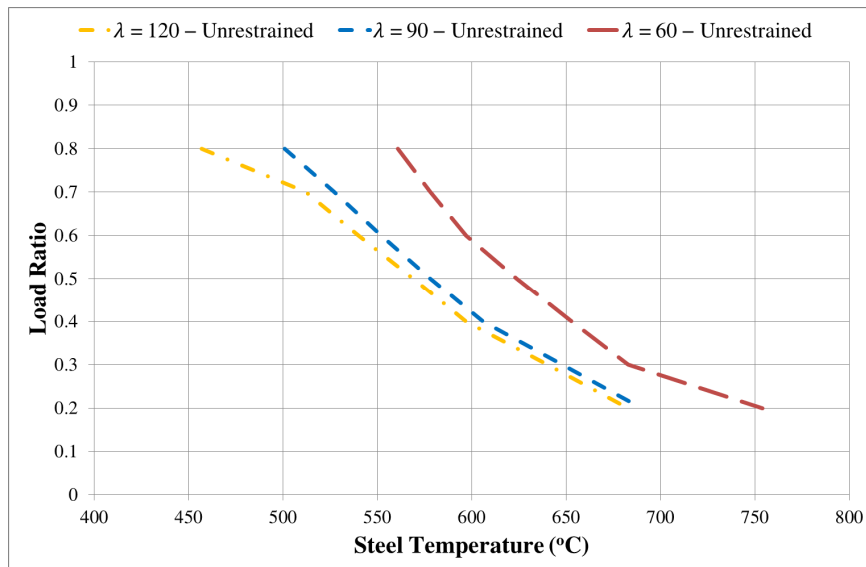Figure 8: Results of parametric analysis for EHS-B for λ=90

Figure 9: Summary of results of parametric analysis for EHS-B for varying slenderness and load ratio

6   Conclusions

By conducting the finite element study, validating the model using the fire tests data, and conducting a parametric analysis the following was found:

- By using variable with temperature thermal expansion coefficient and the EC3 thermal parameters, the FEM model demonstrated an excellent agreement with the experimental temperatures.

11

- Excellent prediction of columns instability. The model has shown outstanding agreement with the tests results for both of the overall and the local buckling modes of failure.
- For the unrestrained models the results are in very good agreement in most cases for the axial displacement.
- The restrained model has also shown a good agreement with the tests results for failure time and displacements.
- The verified finite element model was used to conduct a parametric analysis involving parameters of loading level and slenderness.
- The parametric analysis has shown that the more slender the column the lower the failure temperature.
- The parametric study has shown a non-linear relationship between the loading ratio and the slenderness of the elliptical columns.
- Increasing the loading level form 0.2 to 0.8 has reduced the maximum displacement by 47% and decreased the failure temperature by 28%.
- In columns' slenderness range of 90 to 120 the effect of loading on failure temperature is less than that in the range of 60 to 90.

Acknowledgments

References

[1] T.M. Chan and L. Gardner, Compressive resistance of hot-rolled elliptical hollow sections, Engineering Structures, 30, (2008), 522–532.
[2] Y. Zhu BE and T. Wilkinson, Finite Element Analysis of Structural Steel Elliptical Hollow Sections in Compression, Research Report No R874, February 2007.
[3] N. Jamaluddin, D.Lam and D.Ye, Finite Element Analysis of Elliptical Hollow and Concrete Filled Tube Columns, International Journal of Integrated Engineering (Issue on Civil and Environmental Engineering), 95-101.
[4] BS EN 1991-1-2, Eurocode 1, Actions on structures. General actions. Actions on structures exposed to fire, 2002.
[5] TNO Building and Construction research, DIANA Finite Element Analysis user manuals, release 9.4.3, Delft, 2011.
[6] BS EN 1993-1-2, Eurocode 3, Design of steel structures. General rules. Structural fire design. 2005
[7] EN 1993-1-1. Eurocode 3: Design of steel structures – Part 1–1: General rules and rules for buildings. CEN, 2005.